Effect of organic additives in fluoacid-based Ti and Zr-treatments for galvanized steel on the stability of a polymer coated interface

Fockaert, L. I.; Ankora, M. V.E.; Van Dam, J. P.B.; Pletincx, S.; Yilmaz, A.; Boelen, B.; Hauffman, T.; Garcia-Gonzalez, Y.; Terryn, H.; Mol, J. M.C.

DOI
10.1016/j.porgcoat.2020.105738

Publication date
2020

Document Version
Final published version

Published in
Progress in Organic Coatings

Progress in Organic Coatings 146 (2020) 105738

Contents lists available at ScienceDirect

Progress in Organic Coatings

journal homepage: www.elsevier.com/locate/porgcoat

Effect of organic additives in fluoacid-based Ti and Zr-treatments for galvanized steel on the stability of a polymer coated interface

L.I. Fockaert[a,b], M.V.E. Ankora[b], J.P.B. Van Dam[b], S. Pletincx[c], A. Yilmaz[b], B. Boelen[d], T. Hauffman[c], Y. Garcia-Gonzalez[b], H. Terryn[c], J.M.C. Mol[b,*]

[a] Netherlands Organization for Scientific Research (NWO), Postbus 3021, 3502 GA, Utrecht, The Netherlands
[b] Delft University of Technology, Department of Materials Science and Engineering, Mekelweg 2, 2628 CD Delft, The Netherlands
[c] Vrije Universiteit Brussel, Department of Materials and Chemistry, Research Group Electrochemical and Surface Engineering, Pleinlaan 2, 1050 Brussels, Belgium
[d] Tata Steel IJmuiden B.V., Research and Development, 1970 CA IJmuiden, The Netherlands

ARTICLE INFO

Keywords:
Chemical conversion treatment
Galvanized steel
H_2ZrF_6
H_2TiF_6
Interfacial stability
Adhesion strength
Polyester coil coat

ABSTRACT

The bonding properties of zirconium- and titanium-based conversion coatings were evaluated using model conversion solutions of H_2ZrF_6 and H_2TiF_6 with addition of various organic additives (PAA, PVA, PVP). Macroscopic testing techniques such as contact angle and pull-off adhesion measurements were performed on galvanized steel sheets. Complementary to this, molecular studies were performed on model zinc substrates using ATR-FTIR in the Kretschmann configuration. The macroscopic and molecular approaches showed a good correlation demonstrating ATR-FTIR in the Kretschmann configuration to be a valuable tool to gain fundamental insights in metal oxide-polymer interfacial phenomena. Zirconium-treated galvanized steel substrates were shown to have a higher bonding affinity for the polyester coil coat primer than titanium-treated galvanized steel substrates. The presence of organic additives did not further improve the bonding properties. Yet, organic additives initially improved the interfacial stability of titanium-treated substrates. However, on the long term, organic additives are shown to be detrimental for polyester coil coat adhesion. This adverse effect of organic additives on the long term was assigned to its selective dissolution during immersion and was most pronounced for titanium-treatments. The limited effect of organic additives in case of zirconium-treatments was attributed to the higher portion of chemical interfacial bonds, as well as its tendency for crosslinking reactions causing entanglement of polymeric compounds in the zirconium oxide structure.

1. Introduction

Recent restrictions on the use of carcinogenic hexavalent chromium, as well as ecological concerns on the use of extensive use of phosphates lead to the development of a new generation of surface treatments. [1] Currently, zirconium- and/or titanium-based fluoroacid treatments are considered as viable alternatives since they improve both corrosion resistance [2–7] and paint adhesion [8–12] on both ferrous and non-ferrous substrates [1]. To form a conversion layer, the initial native oxide layer needs to be broken down [13]. In case of zirconium and titanium-based treatments this is done by fluoride ions [14]. During the anodic dissolution of native metal (hydr)oxides, cathodic counter reactions create local surface alkalization, which lead to precipitation of zirconium- and titanium oxide [15–20]. Tetravalent elements are soluble only within narrow acidity ranges and the hydroxides $M(OH)_4$ are too polarized to be stable. [21] Consequently, because of their high formal charge, Ti and Zr cations hydrolyse to hydrated oxides [21,22]. In the case of titanium oxide, spontaneous dehydration via oxolation reactions leads to TiO_2 which crystal structure (rutile or anatase) depends on the acidic and temperature conditions. [14[21,23] Conversely, the high coordination number of zirconium (N_{Zr} = 8 vs N_{Ti} = 6) and resulting geometry (associated with its larger ionic radius) does not allow the formation of compact condensation products.22] Instead, amorphous oxy hydroxides are being formed. [21–25] Literature on precipitation of Zr(VI)- and Ti(VI)-oxides from fluoroacid solutions are very scarce. Verdier et al. showed that during the conversion of AM60 magnesium alloy, titanium occurred only in its oxide form (TiO_2), whereas zirconium, depending on the solution composition, was found as oxide (ZrO_2), oxyhydroxide ($ZrO_{2-x}OH_{2x}$) and hydroxyfluoride. [23] This confirms the formation of amorphous zirconium oxyhydroxide phases, which have been reported to have variable compositions depending on the experimental conditions. [22] As such, the pH, Zr

* Corresponding author.
E-mail address: j.m.c.mol@tudelft.nl (J.M.C. Mol).

https://doi.org/10.1016/j.porgcoat.2020.105738
Received 14 November 2019; Received in revised form 23 April 2020; Accepted 28 April 2020
Available online 28 May 2020

concentration, temperature and presence of anions in the conversion solution determine the equilibrium between competitive olation (leading to Zr − OH-Zr bonds) and oxolation (leading to Zr-O-Zr bonds) reactions. [21,22] Finally, when forming solid phases, OH groups can be replaced by anions, which effect diminishes with increasing pH [22].

Improved paint adhesion has been ascribed to altered oxide physicochemical properties upon zirconium-based treatment. As such, the hydrophilic nature of hot dipped galvanized and Galvan coated steel substrates is reported to increase upon zirconium-based conversion treatment. [26] Increased surface free energies [27], electron donor properties [28,29] and altered hydroxide fractions [11,29,30] have shown to enhance chemical interactions with an organic layer. Molecular studies at buried metal-polymer interfaces require the use of thin organic film or metal substrates. This because industrial coatings and substrates have high absorptive properties, hindering non-destructive access to he buried interface using currently available surface sensitive techniques. Harrick et al, developed attenuated total reflection – Fourier transform infrared spectroscopy (ATR-FTIR) in Kretschmann configuration, thereby demonstrating the feasibility to study the physics and chemistry of optical transparent semiconductor surfaces, by means of total internal reflection [31]. Öhman et al. [32–35] integrated this ATR-FTIR Kretschmann technique with an electrochemical cell (EC), allowing simultaneous electrochemical and molecular characterization of the metal-polymer hybrid system during exposure to electrolyte. Later, Taheri et al. adopted the in-situ ATR-FTIR approach to study molecular organizations at buried metal-polymer interfaces [11,36,37]. Today, ATR-FTIR Kretschmann is a well-established tool to deduce chemisorption mechanisms on polymer coated thermally vaporized model metal substrates [38,39] Nevertheless, its requirement for optical transparent metal substrates comes with the need for complementary methodologies studying (dis)bonding phenomena on industrial relevant substrates. One of these complementary techniques concerns scanning Kelvin probe (SKP) studies allowing for Volta potential surface mappings on industrial metal-polymer hybrid systems. [40,41] Such SKP studies revealed a lowered potential difference at the delamination front reducing the delamination rate [42,43] Next to zirconium and/or titanium, fluoroacid-based treatments typically also contain inorganic and organic additives which affect the conversion oxide physicochemical and thus bonding properties. Inorganic additives are known to improve conversion film formation as well as its barrier properties adding corrosion resistance [5,9,44,45]. However, the impact of organic additives is less described. There are various reasons to add polymeric compounds to the conversion solution. Among others, they are supposed to improve conversion coating homogeneity, as well as enhance bonding properties to both the underlying substrate and overlaying paint layer [46–48]. Common water soluble polymeric compounds found in patents to be added to conversion treatments are polyacrylic acid (PAA), polyvinyl alcohol (PVA) and polyvinyl pyrrolidone (PVP) [47–51]. It has been reported that polymeric additives are more effective in a zirconium- than in a titanium-based coating due to the ability of zirconium to act as a crosslinking agent [46]. Deck et al. reported that the addition of polymeric additives improves both stability and corrosion resistance of zirconium- and titanium-treatment of aluminium, with polyacryl amide performing better than polyacrylic acid [46]. Smit et al. investigated the effect of polyacrylic and tannic acid added to the titanium-treatment of aluminium-manganese alloys and confirmed the corrosion resistance to be improved significantly due to organic additives [52]. However, longer immersion in NaCl solutions leads to selective dissolution of the polymer film resulting in worse corrosion protection performances than those obtained after titanium-treatment without organic additives [52]. Since the majority of the work on zirconium- and titanium-treatments focusses on corrosion resistance and macroscopic adhesion testing, fundamental insights on the bonding properties of zirconium- and titanium coatings are largely missing. Yet similarities can be found in literature describing metal-organic frameworks (MOFs). [53] MOFs are metal ions coordinated to organic ligands forming one, two-or three dimensional structures, mostly containing divalent transition metal cations [53]. However, there is a high interest in increasing the charge of the metal cation to strengthen the cation-ligand bond and thus its chemical stability (especially in the presence of water) [53]. Ti(IV) is considered as a highly attractive, yet challenging cation due to its high polarizing power resulting in fast and spontaneous precipitation of TiO_2 [53]. Zr (IV) on the other hand, has shown to be a noticeable exception for tetravalent cations based MOFs [54]. The high affinity between Zr(IV) and carboxylate oxygen atoms gives stable Zr-MOFs in organic solvents, water and acidic aqueous solutions. In alkaline aqueous solutions they are found to be less stable due to replacement of carboxylate groups by OH^- anions. [54] Although such coordination chemistry cannot fully be translated to metal oxide – polymer interactions, higher bonding properties of zirconium than titanium oxide can be hypothesized from this.

This work aims to describe the chemical conversion of galvanized steel using model conversion solutions. Initially the conversion film formation of galvanized steel is characterized by XPS surface analysis using H_2ZrF_6 and H_2TiF_6 as conversion solution. Subsequently, the bonding properties of the converted oxide surfaces are determined as a function of fluoacid cation (Ti/Zr) and organic additives (PAA, PVP, PVA) using contact angle and attenuated total reflection (ATR)-FTIR measurements. Based on the contact angle measurements the surface free energy of the variously treated galvanized steel substrates is calculated according to the Owens, Wendt, Rabel and Kaelble (OWRK) method, which allows differentiation between polar and dispersive contributions [55]. Complementarily, ATR-FTIR measurements in the Kretschmann configuration elucidate the interface chemistry at the zinc-polyester coil coat interface revealing interfacial bonding mechanisms [56]. In the Kretschmann configuration thin metal films (50 nm) are deposited on an internal reflection element. The metal film thickness is kept sufficiently low to allow access of infrared light through the metal film, providing interfacial molecular information. The use of such inverted geometry offers the possibility to introduce aqueous media to the metal oxide-polymer interface. Consequently, the stability of the established interface can be evaluated in-situ using ATR-FTIR. There has been opted to use deuterated water (D_2O) because the O—D bending mode is positioned at a lower wavenumber compared to the O—H bending mode (i.e. 1200 vs 1640 cm^{-1}, respectively). This shift allows in-situ study of the evolution of interfacial carboxylate bonds positioned around 1610 cm^{-1} without interference of dominant water signals. The evolving interface chemistry elucidated by ATR-FTIR is subsequently correlated to pull-off adhesion measurements obtained after 24 h immersion in an aqueous 0.05 M NaCl solution to study its long term stability.

2. Experimental

2.1. Materials

Hot-dip galvanized steel (GI) sheets with a 15 μm zinc coating and a total thickness of 0.4 mm were sourced from Tata Steel I Jmuiden B. V. They were ultrasonically cleaned in acetone and ethanol both for 10 min. This was followed with an alkaline cleaning step at elevated temperature (60 °C) to remove surface aluminium, which results from the galvanizing process. [57] Therefore, the samples (50 x 50 mm) were immersed for 30 s in 1 M NaOH adjusted to pH 12 using concentrated phosphoric acid, after which they were rinsed using demineralized water and dried with compressed air.

2.2. Conversion treatment

To investigate the effect of the cation (Zr vs Ti) and organic additives, model conversion treatments were prepared. Hexafluorozirconic acid, 50 wt% in H_2O (Sigma-Aldrich Chemistry) and

hexafluorotitanic acid, 60 wt% in H_2O (SigmaAldrich Chemistry) were diluted to 0.01 M. The pH was adjusted to 4 using 1 M NaOH. The polymer additives investigated as potential adhesion enhancers were polyvinyl alcohol (PVA) molecular weight 145 000 (Sigma-Aldrich Chemistry), polyvinylpyrrolidone (PVP) molecular weight 360 000 (Sigma-Aldrich Chemistry) and polyacrylic acid (PAA) molecular weight 150 000 (Sigma-Aldrich Chemistry). They were added to the fluoroacid solutions with a concentration of 0.1 g/L. To dissolve the polymers, stirring at elevated temperatures was required. PVA and PAA were fully dissolved after 30 min stirring at 70 °C, PVP required a higher temperature and was dissolved after 12 h stirring at 80 °C.

2.3. Polymer coating

Samples were polymer coated with a model clearcoat formulation with a polyester-based resin, Dynapol LH 820 (Evonik Industries AG) supplied by AkzoNobel B.V. The hot-dip galvanized steel substrates were spincoated at a speed of 1250 rpm for 40 s, whereafter they were cured at 225 °C for 5 min. The dry film thickness was measured using an Elcometer® 456 coating thickness gauge. The device was first calibrated on uncoated GI using the 'zero' calibration method, which is ideal for calibrating on uncoated smooth surfaces. The average thickness achieved was 10 ± 2 μm. Zinc coated internal reflection elements (IREs) used for attenuated total reflection (ATR)-FTIR studies, were coated using a 30 μm bar coater. The resulting polymer film was cured for 15 min at 130 °C, which is the maximum operating temperature for the germanium IRE.

2.4. Pull-off adhesion test

Pull-off adhesion tests, according to the ASTM D4541-17 standard were performed using the Elcometer® 106 Pull-Off Adhesion tester. Prior to the adhesion testing, coil coated samples were submersed in a 0.05 M NaCl solution for 24 h. Subsequently, 20 mm diameter dollies were attached to each coated sample using SG 300-05 adhesive (SciGrip) and cured for 24 h at room temperature. Prior to testing each sample was glued to a 4 mm thick carbon steel plate with cyanoacrylate adhesive to prevent deformation of the 0.4 mm thick galvanized steel substrates. Subsequently, the polyester coat was cut around the dolly to avoid shear stresses on the dolly-polyester coat bond. The dollies were pulled off at a rate of 10 mPa per second.

2.5. X-ray photoelectron spectroscopy (XPS)

XPS survey spectra were collected using a PHI5600 ci photoelectron spectrometer (Physical Electronics) with an Al Kα monochromatic X-ray source (1486.71 eV of photons). The vacuum in the analysis chamber was approximately 9×10^{-9} Torr during measurements. Measurements were performed with take-off angles of 45° with respect to the sample surface. The reproducibility was verified by triplication of the measurements. XPS data was analysed with PHI Multipak software (V9.1.0.9).

2.6. Field emission auger Electron spectroscopy (FE-AES)

High-resolution mappings of the zirconium- and titanium treated galvanized steel substrates were obtained using a JEOL JAMP9500 F FE-AES spectrometer, employing an electron beam of 10 keV and 10.6 nA at an angle of incidence of 30°. The utilized magnification was 12,220 x for zirconium-treated GI and 20,000 x for titanium-treated GI. This resulted in mapping areas of approximately 9 x 9 μm for zirconium-treated GI and 6 x 6 μm for titanium-treated GI. The data was extracted and processed using the JEOL Image Investigator V1.04 software.

2.7. Contact angle measurements

Contact angle measurements of variously treated GI were performed using a OneAttension Theta Lite optical tensiometer (Biolin Scientific). Milli-Q water, ethylene glycol and diiodomethane were the liquids used to calculate dispersive and polar parts of the surface free energy (SFE). The procedure involved placing a drop of liquid with a volume of 1.5 μL on the surface of the sample, whereafter wetting force data were recorded for 10 s starting from the moment of liquid contact. The contact angle at the metal-liquid-air interface obtained after 10 s of contact with the solid substrate is presented in this work. SFE values were calculated based on the OWRK method using the OneAttension software. The reproducibility was verified by at least five measurements per liquid and substrate, of which the values and their associated standard deviations can be found in supplementary information. The average contact angle value for each liquid/substrate was used for calculating the SFE.

2.8. Attenuated total reflection – Fourier transform infrared spectroscopy (ATR-FTIR) in Kretschmann configuration

The FTIR apparatus was a Thermo-Nicolet Nexus equipped with a liquid-nitrogen cooled mercury-cadmium-telluride (MCT) detector and a nitrogen-purged measurement chamber with a Veemax III single reflection ATR accessory with a mounted precision manual polarizer (PIKE) set at 90° for p-polarized IR-light. Metallic zinc films were deposited on germanium IREs with a fixed face angle of 60 degrees (PIKE Technologies) using pure zinc foil (Goodfellow, 99.95%) by means of a high-vacuum (VCM 600 Standard Vacuum Thermal Evaporator, Norm Electronics) evaporation system. The acquired zinc film thickness was equals 50 nm and was measured by means of a quartz microbalance thickness meter implemented in the PVD equipment. Because of the high purity grade of the zinc source, there was no need to apply an alkaline treatment prior to conversion. Yet, it should be noted that ATR-FTIR measurements require the use of thermally vaporized model substrates which differ from industrial galvanized steel substrates. Variations are expected on the activity of the metal oxide layer, initial and final hydroxide fractions and the thickness of the conversion oxide layer. Nonetheless, complementary ATR-FTIR measurements are able to provide complementary insights in the chemisorption mechanisms at variously treated buried zinc-polyester interfaces, which accordingly can be associated to the characteristics of variously treated galvanized steel substrates. P-polarized IR-light was configured with an incident set angle of 80 degrees. For the chemisorption studies infrared backgrounds were obtained from the variously treated metallic coat films deposited on IREs. For the stability studies, infrared backgrounds were obtained after curing the polyester coil coat coating on the respective metal oxides. The established interfacial chemistry was followed in-situ during exposure to D_2O (99.9%, Sigma-Aldrich Chemistry). Consequently, the evolution of interfacial bonds may appear positive, when being increased, or negative when being reduced relative to the initial dry (cured) situation. Infrared spectra were collected every 300 s and averaged from 128 cycles with a resolution of 4 cm^{-1}. The control of the spectra acquisition and incident angles was managed by the OMNIC 8.1 software package (ThermoElectron Corporation, Madison, WI).

3. Results

3.1. Formation of zirconium- and titanium-based conversion coatings

3.1.1. Elemental surface analysis, XPS and FE-AES study

The formation of a zirconium- and titanium-based conversion film on GI was studied using XPS. The survey spectrum of untreated GI, presented in Fig. 1(a), includes XPS peaks for oxygen, zinc, aluminium and carbon. The presence of aluminium on untreated GI indicate that

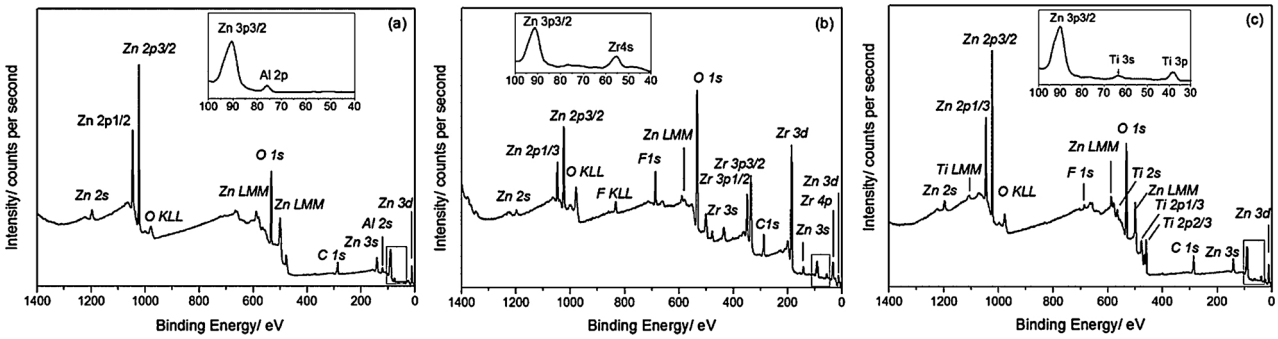

Fig. 1. XPS survey scans of conventional galvanized steel GI, (a) without chemical conversion treatment (b) after zirconium-treatment and (c) after titanium-treatment.

the applied alkaline cleaning procedure does not remove all surface aluminium. However, subsequent zirconium- and titanium-treatment efficiently removes remaining surface concentrations of aluminium, as demonstrated in Fig. 1(b) and (c). Based on the zirconium-based conversion mechanism proposed by Lostak et al. [19] it is suggested that the zinc matrix is more noble compared to the aluminium impurities. Hence, these aluminium impurities are being dissolved, while zirconium oxide precipitates covering the galvanized steel surface. Previous work compared polyester coil coat chemisorption mechanisms on native and zirconium-treated zinc and aluminium, which becomes important when substantial concentrations of aluminium remain present at industrial relevant galvanized steel surfaces [39].

Furthermore, zirconium, titanium and fluoride XPS peaks were detected in the relevant oxides, as shown in Fig. 1(b) and (c).

The elements traced in the XPS survey scans were converted to atomic percentages using the sensitivity factors (S) provided by the manufacturer. [58] It is known that the overlayer of ambient carbon contaminants attenuates signals from the underlying surface [59]. As a consequence, carbon and oxygen signals are predominant as illustrated in Fig. 2(a). Furthermore, higher levels of fluorides are noted upon zirconium- compared to titanium-treatment. The metal concentrations at the variously treated galvanized steel surfaces are presented in Fig. 2(b). This shows that aluminium concentrations are being reduced from 7.2 ± 0.4 At. % for untreated GI to 0.9 ± 0.3 At. % for zirconium-treated GI and 0.4 ± 0.4 At. % for titanium-treated GI. Moreover, it can be seen that the amount of surface zinc reduces, while zirconium (14.0 ± 2.1 At. %) and titanium concentrations (9.6 ± 1.5 At. %) increases. Nevertheless, significantly higher zinc concentrations are noted after titanium-treatment which suggests that the zirconium-based conversion coating is either thicker or more homogeneous than the titanium-based conversion coating.

To study the lateral elemental distribution of the converted GI substrates FE-AES mappings were performed. Fig. 3(a) and (b) demonstrate the lateral zinc and zirconium distribution of zirconium-treated GI, whereas (c) and (d) present the lateral zinc and titanium distribution at the titanium-treated GI surface. The absence of surface zinc at the zirconium-treated GI surface, as shown in Fig. 3(a), illuminates that zirconium-treated GI is homogeneously covered by zirconium oxide. Conversely, elemental AES mappings of titanium-treated GI demonstrates comparable surface concentrations of zinc and titanium oxide. Consequently, whereas zirconium-treated GI results in a homogeneous zirconium oxide layer, titanium-treated GI results in a heterogeneous conversion oxide layer, containing both titanium- and zinc oxide. The higher zinc concentration after titanium-treatment shown by XPS analysis in Fig. 2(b), is thus clearly associated with a heterogeneous surface. Meanwhile, FE-AES mappings illustrate negligible zinc concentrations at the outer zirconium oxide surface. Since, significant concentrations of zinc (6.0 ± 1.7 At. %) were probed by means of XPS after zirconium-treatment of GI, as shown in Fig. 2(b), this infers that the respective zirconium oxide layers are thinner than the sampling depth for XPS for AlKα radiation, which is known to situate between 3 and 10 nm. [60]

3.2. Bonding properties of zirconium- and titanium-based conversion coatings

3.2.1. Contact angle studies on surface free energy (SFE)

The resulting surface free energies of variously treated GI substrates obtained using the OWRK method are presented in Fig. 4(a) and (b), respectively. Measured contact angle values, their averages and standard deviations are presented as supplementary information and indicative for the reproducibility of the data shown in Fig. 4. The total SFE (γ^{tot}) includes both dispersive (γ^{d}) and polar contributions (γ^{p}). The former reflects van der Waals and London interactions, whereas the

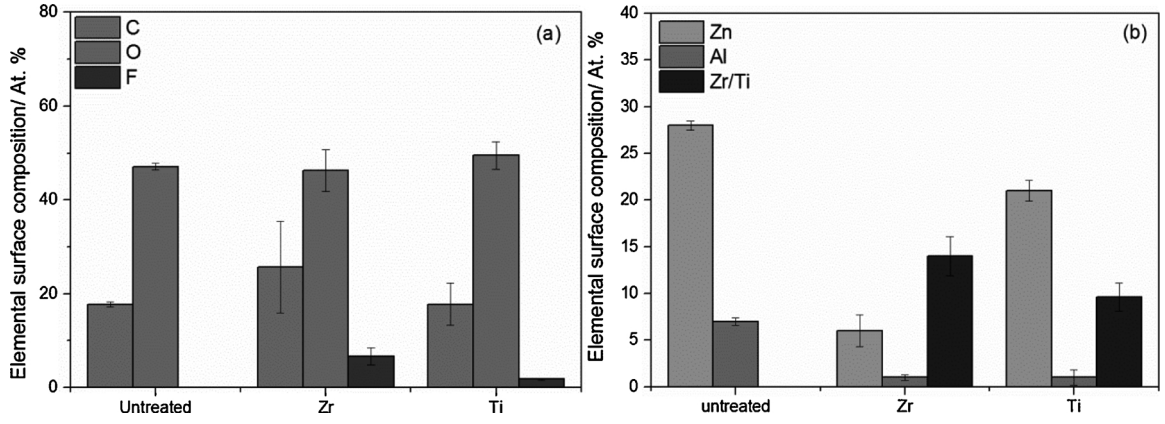

Fig. 2. Elemental composition of variously treated GI, based on XPS surface analysis (a) carbon, oxygen and fluoride contributions (b) metal contributions; zinc, aluminium, magnesium, zirconium and titanium.

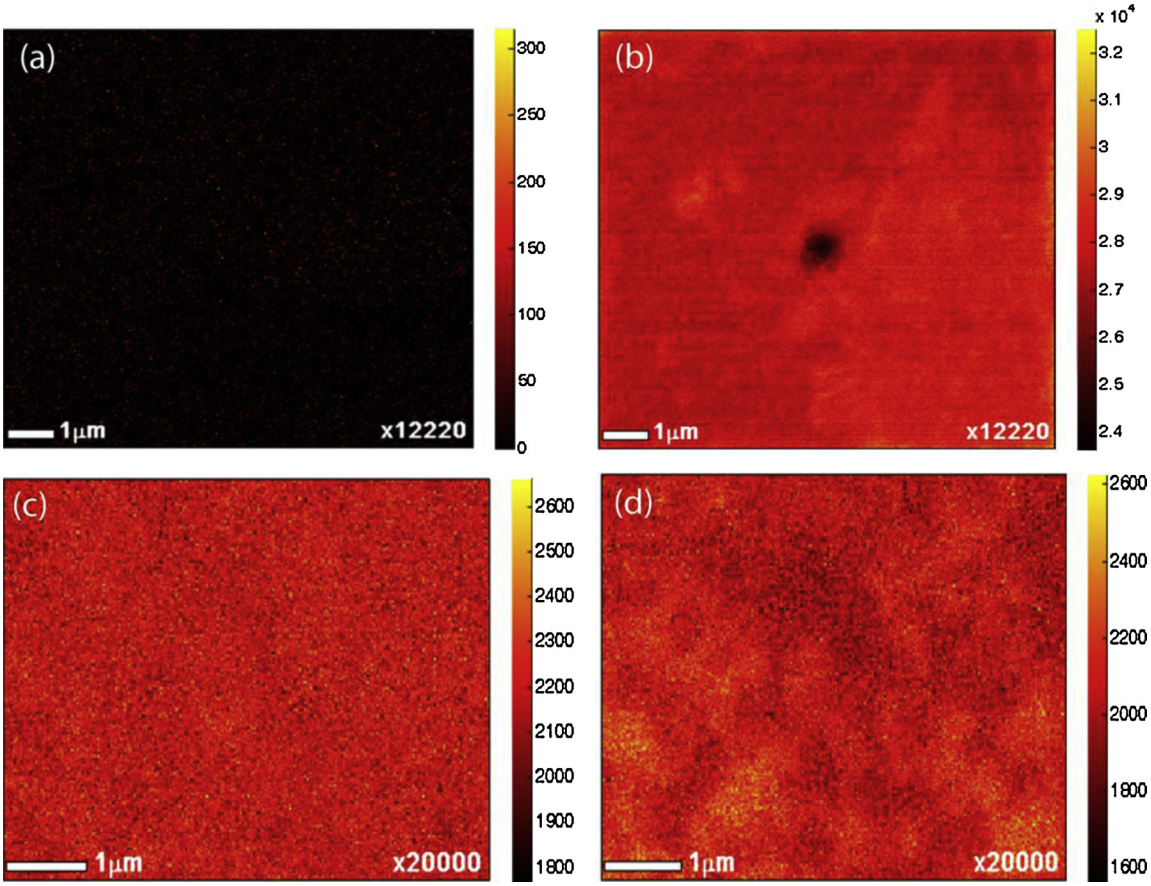

Fig. 3. FE-AES elemental mappings of zirconium-treated GI with (a) zinc and (b) zirconium mappings and titanium-treated GI with (c) zinc and (d) titanium mappings.

latter represents acid-base and hydrogen interactions. [55,61] It can be seen that the dispersive forces (35.0 ± 3.3 mN/m) on GI remain more or less unaffected upon the various conversion treatments. Contrary, the polar SFE of untreated GI (2.2 mN/m) increases by approximately a factor ten after both zirconium- and titanium-treatment without organic additives (25.3 mN/m and 21.9 mN/m, respectively). This increase in polar forces is associated with the high valence number of Zr(IV) and Ti (IV) increasing the surface oxide polarizing power and thus its chemical activity [53]. However, the addition of polymeric compounds to the zirconium-treatment does not give any further increase in polar surface forces. Similar surface free energies are noted after adding PAA and PVA, whereas a reduction in polar surface forces can be seen after adding PVP to the zirconium-treatment, as shown in Fig. 4(a). More distinct variations in chemical polarity due to organic additives are evidenced in case of titanium-treated GI, shown in Fig. 4(b). The addition of PAA slightly increases polar surface forces. However, an obvious reduction in chemical polarity is noted with PVA and PVP additions. Nonetheless, dispersive forces remain equal to those obtained for untreated GI.

3.2.2. ATR-FTIR studies on interfacial bonding mechanism

The effect of chemical conversion treatment on the molecular organisation at the polymer – metal interface is studied using ATR-FTIR in Kretschmann configuration. Fig. 5 illustrates ATR-FTIR spectra obtained without metallic film (blank), native zinc oxide (Zn), titanium-treated zinc (Zn Ti) and zirconium-treated zinc (Zn Zr). The blank ATR-

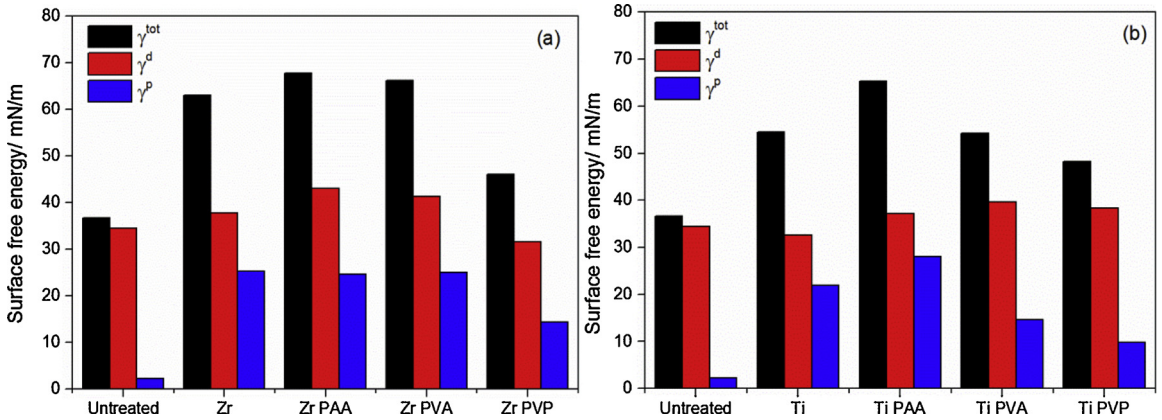

Fig. 4. Surface free energies of (a) zirconium- and (b) titanium-treated GI.

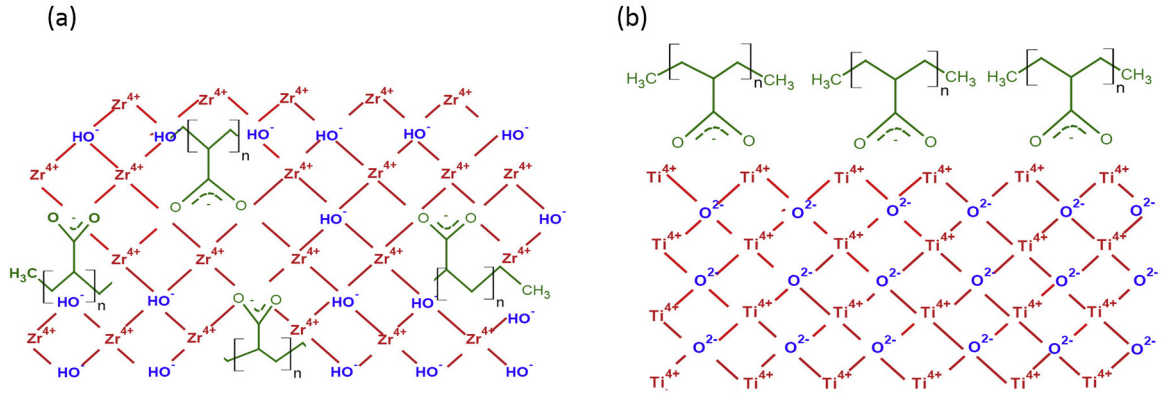

Fig. 5. (a) ATR-FTIR spectra of cured polyester coating applied on blank IRE (without zinc film) and variously treated zinc substrates (b) zoom in polyester coating interaction with variously treated zinc substrates.

FTIR spectrum of cured polyester coating is characterized by a strong peak at 1715 cm^{-1} assigned to C═O stretch vibrations, a small sharp peak at 1605 cm^{1} attributed to aromatic ring stretching vibrations and a peak at 1550 cm^{-1} assigned to ring vibrations specific to the melamine-based crosslinker. [62] Additional peaks in the lower wavenumber region are attributed to the polymer backbone of both the polyester resin and the melamine-based crosslinker, as well as fillers present in the paint formulation [62]. It can be seen that upon interaction with variously treated zinc substrates the peak at 1605 cm^{-1} appear more broad and intense. Since aromatic ring vibrations do not broaden in FTIR spectra, this band is ascribed to asymmetric carboxylate (COO^{-}_{as}) stretching vibrations associated to the formation of a newly formed interfacial bond. [62,64] Furthermore, the carbonyl peaks observed on zirconium- and titanium-treated zinc are positioned at higher wavenumbers (1726 and 1729 cm^{-1}, respectively) compared to untreated zinc (1714 cm^{-1}). From the coil coat formulation it is known that the polyester resin contains both acid and ester functional groups, which leads to two contributions at the carbonyl peak. Since ester carbonyl bonds vibrate at higher wavenumbers (> 1720 cm^{-1}) [63] compared to acid carbonyl bonds (< 1720 cm^{-1}), [63] this shift towards higher wavenumbers indicates a reduced fraction of acid carbonyl bonds at the conversion treated zinc interface. Consequently, protonated acid groups (COOH) are being converted to deprotonated carboxylate groups (COO^{-}) at the zinc surface forming interfacial carboxylate bonds, which is in accordance with the appearance of a broad carboxylate peak at 1605 cm^{-1}. A similar bonding mechanism, i.e. interfacial carboxylate bond formation with carboxylic groups specific to the polyester resin, is thus revealed on both the native zinc oxide surface as well as the zirconium- and titanium-treated zinc surfaces. Yet, a lower carbonyl (C═O) and higher carboxylate (COO^{-}_{as}) peak intensity can be observed for zirconium-treated compared to titanium-treated substrates. This demonstrates a higher affinity of zirconium oxide for carboxylates bond formation with the polyester resin. On the other hand, the shoulder attributed to C–N = C bonds of the melamine-based crosslinker is more pronounced at titanium-treated zinc substrates. This increase in melamine (C–N = C) peak intensity is associated to a higher bonding affinity of titanium-treated zinc for the melamine-based crosslinker. The mechanism of interfacial interactions between metal oxide and melamine-based crosslinkers have been reported previously [39].

Fig. 6(a) and (b) show the obtained interfacial chemistry between variously treated zinc substrates and the polyester coating upon adding the polymeric compounds of interest (PAA, PVA and PVP) to the zirconium- and titanium–treatments respectively. It should be noted that these spectra were collected using the conversion treated zinc substrates as a background, which means that the chemical structures associated with the organic additives are included in the background. Despite the inclusion of organic additives in the background, it can be seen from Fig. 6(a) that the carbonyl (C═O) peak intensity of polyester coated zinc increases for zirconium-treatments containing organic additives compared to zirconium-treated zinc without organic additives as shown in Fig. 5. This higher C═O peak refers to more carboxylic groups (COOH or COOR) at the converted oxide interface which are not involved in interfacial carboxylate bond formation (COO^{-}). Consequently, the presence of organic additives does not further improve the bonding properties of zirconium oxide, which agrees with the similar or lowered polar component of the SFE given in Fig. 4(a).

To verify the degree of interfacial bond formation the COO^{-}_{as}/C═O peak area ratio is calculated, which requires deconvolution of the carboxylate peak into its two components, being COO^{-}_{as} and C–N = C. This was done using the following fitting parameters: (1) COO^{-}_{as} subpeak centered at 1595 ± 6 cm^{-1}, with a FWHM of 56 ± 4 cm^{-1} and (2) C–N = C subpeak centered at 1552 ± 10 cm^{-1}, with a FWHM of 25 ± 3 cm^{-1}.

Fig. 7 presents the COO^{-}_{as}/C═O and COO^{-}_{as}═/C–N = C peak area ratios, based on the peak areas presented in Fig. 6(a) and (b). The resulting COO^{-}_{as}/C═O peak area ratio, shown in Fig. 7(a) represents the affinity of the conversion treated zinc substrates for carboxylate bond formation. The higher this ratio, the more carboxylate bonds are being formed at the respective oxide surface. Consequently, zirconium-treated zinc substrate possess a higher carboxylate bonding affinity compared to titanium-treatment. Yet, the presence of organic additives does not further enhance carboxylate bond formation. On the contrary, PAA and PVA are shown to reduce the chemical reactivity of zirconium oxide. From the obtained COO^{-} and C–N = C peak areas, competitive interfacial interactions with polyester resin and melamine-based crosslinker were verified using the COO^{-}_{as}/C–N = C peak area ratios, as presented in Fig. 7(b). The lower COO^{-}_{as}/C–N = C peak area ratios for titanium-treated zinc substrates refer to a higher bonding affinity for the melamine-based crosslinker compared to zirconium-treated zinc substrates. This bonding affinity for melamine-based crosslinker appears to be further enhanced by adding organic additives to the titanium-treatment.

3.3. Effect of zirconium- and titanium-based conversion coatings on the interfacial stability in an aqueous environment

3.3.1. In-situ ATR-FTIR study on chemical interfacial bond degradation in the presence of D_2O

The stability of established interfacial bonds on variously treated zinc substrates was evaluated during immersion in aqueous environment. To avoid interference in the carboxylate region from O–H bending vibrations, polyester coated substrates were exposed to D_2O. [39] A background was collected after curing of the polyester coating on variously treated zinc surfaces. Therefore, all positive FTIR signals during immersion represent additional chemical bonds in the interfacial region, whereas negative signals are attributed to a loss of chemical bonds with respect to the dry state. Fig. 8(a) shows in-situ ATR-FTIR

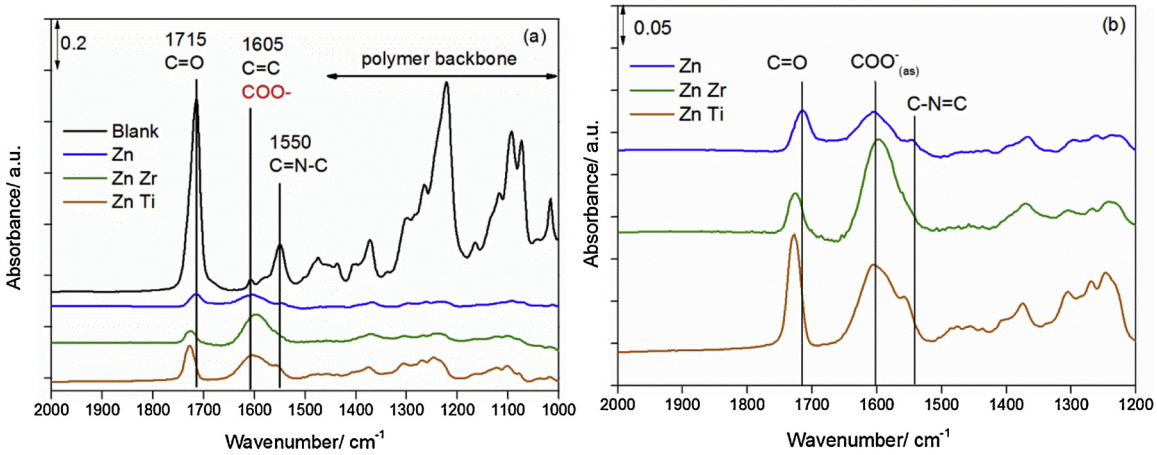

Fig. 6. ATR-FTIR spectra of cured polyester coating applied on (a) zirconium-treated zinc and (b) titanium-treated zinc substrates.

spectra of zirconium-treated zinc. Two distinct phases can be differentiated. Initially, the intensity of the asymmetric carboxylate peak positioned at 1611 cm^{-1} increases, referring to an increasing number of interfacial carboxylate bonds. This increase in carboxylate bond formation can be explained by the introduction of D_2O at the interface encouraging ester hydrolysis and thus forming more reactive carboxylic acid species. [38,64,65] In case of zirconium-treated zinc, maximum $COO^-_{(as)}$ peak intensity is noted after 2.5 h of exposure to D_2O, indicated by the blue curve. Subsequently, the asymmetric carboxylate peak gradually reduces while shifting towards lower wavenumbers. This shift indicates weakening of interfacial bonds and thus an early state of disbondment. [66] Therefore, the real onset of disbondment occurs when maximum carboxylate peak intensities start reducing again, as depicted in Fig. 8(b). Finally, after 5.5 h the asymmetric carboxylate peak area turns to zero. Longer immersion times result in negative peak areas indicating loss of chemical interfacial bonds as compared to the dry state to which the in-situ spectra are normalized. Therefore, this point at 5.5 h in the case of zirconium-treated zinc is defined as the onset of disbondment.

The immersion times required to observe disbondment (COO^-_{as} peak area equal to zero) on variously treated zinc substrates, are summarized in Fig. 9. Zirconium-treated zinc appears to improve the interfacial stability of polyester coated zinc more efficiently than titanium-treated zinc. On the other hand, the effect of organic additives added to zirconium-treatments is less pronounced than when added to titanium-treatments. Comparing the three additives, PAA yields the best performance in stabilizing the zinc-polyester interface in presence of D_2O. PVA and PVP are shown to improve interfacial stability when added to titanium-treatment, but slightly reduce interfacial stability when added to zirconium-treatment.

3.3.2. *Pull-off adhesion tests*

Pull-off adhesion tests have been performed after 24 h immersion of polyester coated substrates in 0.05 M NaCl solution, which results are given in Fig. 10. A pull-off failure stress of 7.2 ± 1.6 MPa was noted for untreated GI. After zirconium- and titanium-treatment the pull-off failure stress increased to 9.3 ± 1.6 MPa and 8.6 ± 1.3 MPa, respectively. The larger increase in adhesion strength in the case of zirconium-treatment (± 30%) compared to titanium-treatment (± 20 %) is in line with the higher polar contribution of SFE demonstrated in Fig. 4 and the higher elemental concentration of Zr compared to Ti shown in Fig. 2(b).

Adding polymeric compounds to both zirconium- and titanium-treatment reduces the adhesion strength. This is most obvious for the titanium-treatment of GI which gives an adhesion strength of 8.6 ± 1.3 MPa without organic additives and 5.0 ± 0.8 MPa with organic additives. Consequently, the adhesion strength reduced significantly after 24 h of immersion in aqueous environment. With a reduced failure stress of ca. 42 % for titanium-treated zinc and ca. 13 % for zirconium-treated zinc upon the addition of organic additives. In contrast to the initial advantageous effect of the polymeric compounds added to the titanium-treatment demonstrated by ATR-FTIR, the final adhesion strength after longer immersion times becomes thus even worse than untreated GI.

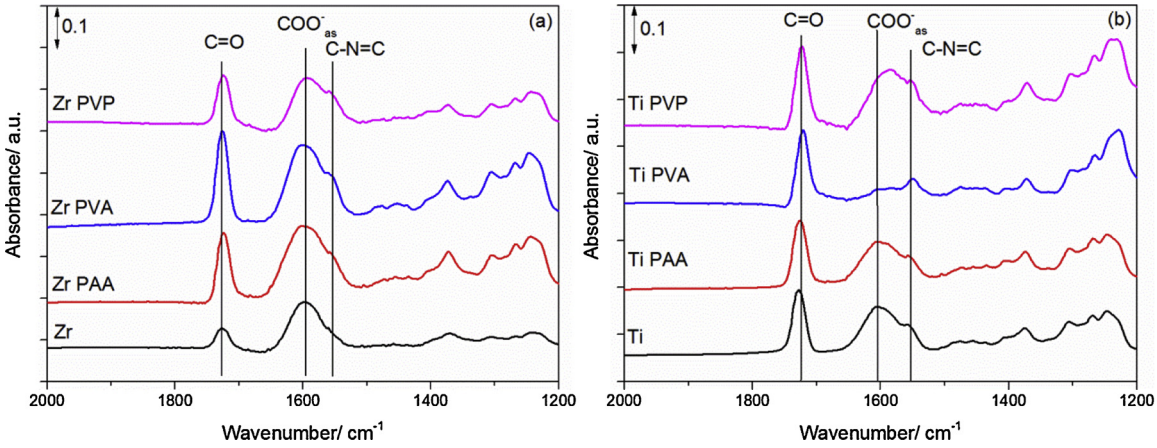

Fig. 7. ATR-FTIR peak area ratio obtained for variously treated zinc substrartes (a) COO^-_{as}/C=O ratio representative for carboxylate bond formation with polyester resin, (b) COO^-_{as}/C = N–C ratio representative for competitve interaction with melamine-based crosslinker.

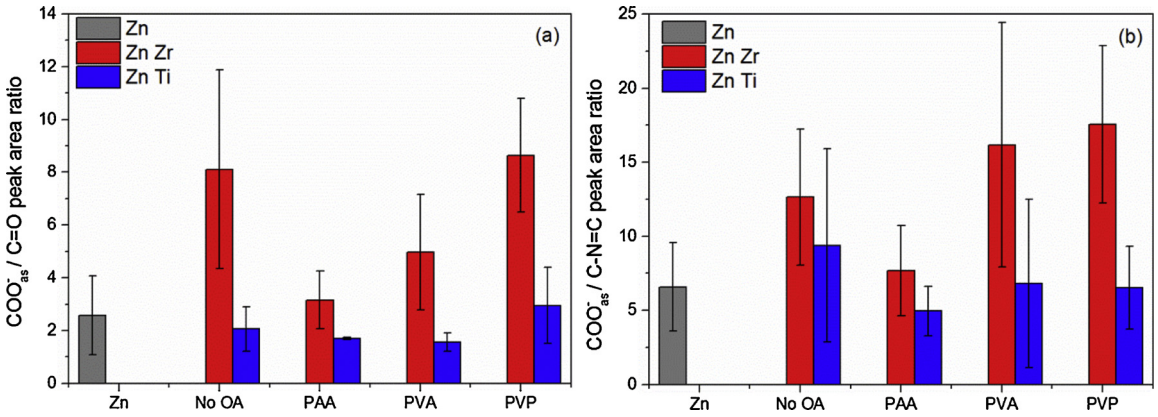

Fig. 8. in-situ ATR-FTIR spectra of zirconium-treated zinc with 30 μm polyester coat as a function of exposure time to D_2O.

4. Discussion

It was shown that Zr- and Ti-based conversion treatment mainly affects the polar part of the SFE, whereas dispersive forces remain more or less equal to untreated GI. This increase in polar forces is associated with the high valence number of Zr(IV) and Ti(IV) increasing the surface oxide polarizing power and thus its chemical activity. [53] This explains the higher bonding affinity for polyester coil coat upon zirconium-and titanium-treatment of zinc compared to untreated zinc.

However, the addition of polymeric compounds to the zirconium-treatment does not give any further increase in polar surface forces. On the contrary, in the case of PVA and PVP polar surface forces are even being reduced, which is far more pronounced for titanium-treatment compared to zirconium-treatment. Moreover, interfacial ATR-FTIR chemisorption studies demonstrated that the presence of organic additives does not further improve the bonding properties of zirconium- and titanium oxide, which agrees with the reduced polar component of the SFE.

Whereas the SFE greatly alters upon adding organic additives to the titanium-treatment, variations in SFE are much more limited when adding those organic additives to zirconium-treatment. It is suggested that the limited impact of organic additives on the SFE of zirconium-treated GI relates to the tendency of zirconium to precipitate as an amorphous oxyhydroxide inducing crosslinking reactions with the polymeric compounds. [22] This is expected to result in entanglement of the additives within the zirconium oxide layer [23,46]. On the other hand, titanium oxide is thermodynamically stable in a crystalline oxide structure and does not show these crosslinking capacities [21]. As a result, separated layers of titanium oxide covered by a polymeric films

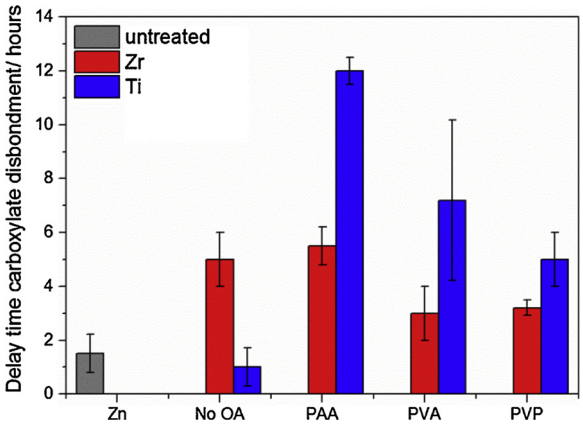

Fig. 10. Pull-off adhesion strength of polyester coating to GI as a function of chemical conversion treatment.

are expected, which might explain the higher impact of organic compounds on the SFE of titanium-treated GI. The proposed oxide structures are given in Fig. 11]. Although the crosslinking capacities of zirconium, as well as the different nature of precipitation products when comparing zirconium- and titanium oxide have been frequently reported. [21,23,46] Experimental validation of the entanglement of organic additives in the conversion oxide structures is highly challenging. This because the precipitated oxide layers are rather thin (25–50 nm). Dominating mixing effects during depth profiling might induce preferential sputtering, which affects the shape of the depth profile. [67] Therefore, acquired sputter profiles will be hard to interpret which is

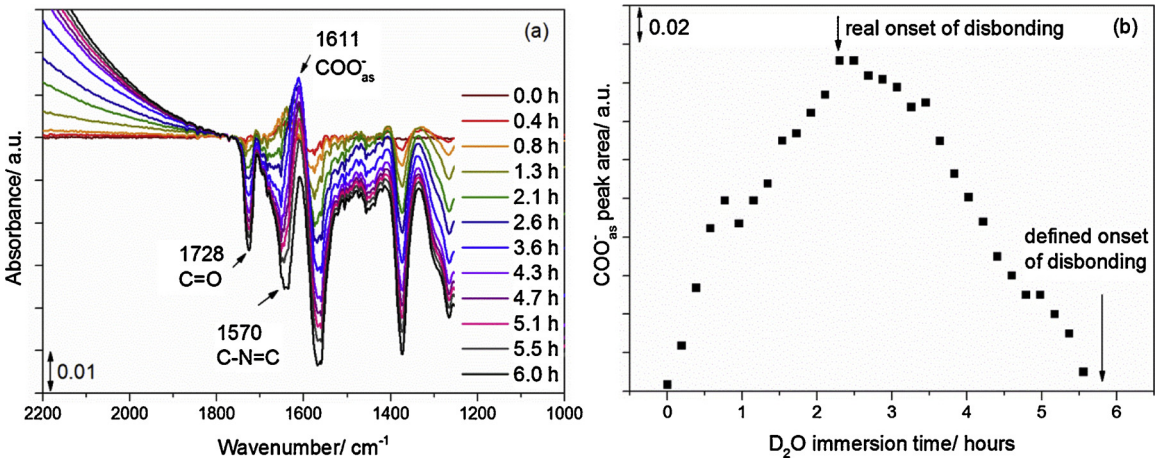

Fig. 9. Delay time for carboxylate disbondment during immersion in D_2O, observed using in-situ ATR-FTIR.

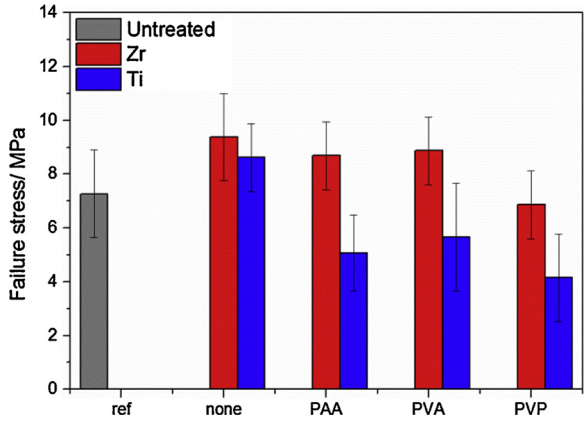

Fig. 11. Proposed conversion oxide structures containg PAA as organic additive, (a) PAA crosslinked in amorphous zirconium-oxide strucure, (b) PAA as covering layer on top of crystaline titanium oxide structure.

further complicated by the coexistence of carbon signal associated to ambient contamination [67,68]. Especially, small fatty acids strongly adsorb to metal oxide surfaces upon immediate contact to atmospheric environment, which hinders unambiguous assignment of carbon signal to the respective organic additives [69,70].

The entanglement of organic compounds into the zirconium oxide structure, as shown in Fig. 11(a), reduces available Zr^{4+} cationic bonding sites, which is held responsible for the lower binding affinity of zirconium-treated zinc upon adding organic additives. For titanium-treated zinc, carboxylate bonding affinity did not alter upon adding organic additives. However, a higher portion of C–N = C bonds were noted associated to a higher amount of melamine-based crosslinker at the titanium-treated interface. It is well-known that titanium due to its small ionic radius is even more acidic than zirconium [21]. Consequently, due to its high positive partial charge, its tendency to donate hydroxide ions is very low. Because of this, electrostatic interactions with the highly polarized titanium oxide structure and electron-rich nitrogen ring structures are hypothesized as favoured interaction mechanism. Previous work demonstrated that electrostatic interactions between metal oxides and electron-rich ring structures can play a predominant role in interfacial metal-molecule interactions since they were held responsible for the in-plane orientation of the carboxylic bonds [71]. A comparable interaction mechanism is proposed between titanium-treated zinc substrates and the electron-rich ring structures of the melamine-based crosslinker.

During ATR-FTIR studies it becomes clear that the effect of organic additives on the interfacial stability of carboxylate bonds is susbtantially more pronounced when added to the titanium-treatment, compared to zirconium-treatment. However, ATR-FTIR studies in dry consitions elucidated electrostatic interactions with melamine-based crosslinker as major bonding mechanism for titanium-treated zinc substrates. Therefore, improved carboxylate bond formation during wet conditions might be associated to initial dissolution of organic additives, followed by carboxylate bond formation between hydrated polyester resin and hydroxylated titanium oxide.

Nevertheless, this initial positive effect of organic additives on the delay time for carboxylate disbondement canot be extended to the long term macroscopic stability of titanium-treated GI. Pull off testing after 24 h submersion in 0.05 M NaCl solution demonstrated reduced failure stresses of 13 % and 42 % due to the presence of organic additives at zirconium- and titanium treatments, respectively. As illustrated in Fig. 11(b), the lack of crosslinking ability of titanium oxide is expected to result in more discrete layers of polymeric compounds and titanium oxide. Because of this, added organic compounds becomes more susceptible to dissolution in aqueous environments. Conversely, in the case of zirconium-treatment, organic additives are expected to be entangled in the zirconium oxide structure, which limits their impact on interfacial stability. It is expected that these variations in conversion oxide layer-build, are responsible for the various impact of organic additives on the interfacial stability of zirconium- and titanium-treated zinc substrates. Moreover, titanium-treatment of zinc increases electrostatic interactions with the melamine crosslinker of the polyester coil coat, which are more sensitive to water replacement, compared to chemical carboxylate bond formation.

5. Conclusions

The formation of zirconium and titanium oxide layers on GI from model conversion solutions without additives was evidenced by XPS and FE-AES surface analysis. It was shown that both zirconium- and titanium-treatment increased the polar component of the SFE by a factor ten, improving polar interactions across the interface. In line with this, ATR-FTIR studies demonstrated increased carboxylate bond formation upon zirconium- and titanium-treatment. However, adding polymeric compounds to the conversion solutions did not further enhance interfacial bond formation. On the other hand, interfacial stability of zinc upon titanium-treatment containing organic additives was shown to increase during initial exposure in aqueous environment. Nevertheless, after 24 h exposure to an aqueous environment, the pull-off adhesion strength significantly reduced due to addition of polymeric compounds to the titanium-treatment. This disadvantageous effect was associated to the selective dissolution of polymeric compounds during immersion. Consequently, although organic additives initially improve interfacial stability, their presence becomes detrimental during prolonged immersion. This adverse effect was most obvious for titanium-treatment compared to zirconium-treatment, giving a reduced adhesion strength of 40 and 14 %, respectively. The lower impact of organic additives in case of zirconium-based conversion coatings was attributed to the entanglement of organic compounds in the zirconium oxide structure as well as to the higher portion of chemical interfacial bonds. Variations in stability of titanium versus zirconium-based conversion coatings with organic additives, are thus associated to different precipitation properties of these tetravalent cations, resulting in a different conversion layer build-up and interfacial bonding properties. Further research is required to develop a surface sensitive approach to accurately determine the layer composition of these ultrathin conversion coatings.

Credit author statement

L.I.F. wrote the main manuscript text, M.V.E.A., J.P.B.V.D., S.P., A.Y., B.B., T.H., Y.G., H.T. and J.M.C.M. all reviewed the manuscript text.

Declaration of Competing Interest

The authors declare that they have no known competing financial interests or personal relationships that could have appeared to influence the work reported in this paper.

Acknowledgements

This research was carried out under project number F81.3.13509 in the framework of the Partnership Program of the Materials innovation institute M2i (www.m2i.nl) and the Foundation for Fundamental Research on Matter (FOM), which is part of the Netherlands Organisation for Scientific Research NWO (www.nwo.nl). S.P. acknowledges financial support by Research Foundation-Flanders (FWO) under project number SB-19-151. M.V.E.A. acknowledges financial support by Materials innovation institute M2i under project number S17003 J.P.B.D. acknowledges financial support by Materials

innovation institute M2i and Technology Foundation TTW (www.stw.nl), which is part of the Netherlands Organization for Scientific Research under project number S32.4.14552b. A.Y. acknowledges financial support by Materials innovation institute M2i and the Foundation for Fundamental Research on Matter (FOM) under project number F41.3.14546a. The authors would also like to acknowledge Gavin Scott from AkzoNobel for the primer formulations.

Appendix A. Supplementary data

Supplementary material related to this article can be found, in the online version, at doi:https://doi.org/10.1016/j.porgcoat.2020.105738.

References

[1] I. Milošev, G.S. Frankel, Review—conversion coatings based on zirconium and/or titanium, J. Electrochem. Soc. 165 (3) (2018) C127–C144.
[2] G. Yoganandan, K. Pradeep Premkumar, J.N. Balaraju, Evaluation of corrosion resistance and self-healing behavior of zirconium-cerium conversion coating developed on AA2024 alloy, Surf. Coatings Technol. 270 (2015) 249–258.
[3] N.W. Khun, G.S. Frankel, Composition and Corrosion Protection of Hexafluorozirconic Acid Treatment on Steel, Mater. Corros. 66 (11) (2015) 1215–1222.
[4] H. Ardelean, I. Frateur, P. Marcus, Corrosion protection of magnesium alloys by cerium, zirconium and niobium-based conversion coatings, Corros. Sci. 50 (7) (2008) 1907–1918.
[5] A. Ghanbari, M.M. Attar, Influence of phosphate ion on the morphology, adhesion strength, and corrosion performance of zirconium-based surface treatment, J. Coatings Technol. Res. (2015).
[6] R.R. Pareja, R.L. Ibáñez, F. Martín, D. Leinen, Corrosion behaviour of Zirconia barrier coatings on Galvanized steel, Surf. Coat. Technol. 200 (2006) 6606–6610.
[7] L. Fedrizzi, F. Rodriguez, S. Rossi, F. Deflorian, R. Di Maggio, The use of electrochemical techniques to study the corrosion behaviour of organic coatings on steel pretreated with Sol–Gel Zirconia films, Electrochim. Acta 46 (2001) 3715–3724.
[8] S. Sharifi Golru, M.M. Attar, B. Ramezanzadeh, effects of surface treatment of aluminium alloy 1050 on the adhesion and anticorrosion properties of the epoxy coating, Appl. Surf. Sci. (345) (2015) 360–368.
[9] H.R. Asemani, P. Ahmadi, A.A. Sarabi, H. Eivaz Mohammadloo, Effect of zirconium conversion coating: adhesion and anti-corrosion properties of epoxy organic coating containing zinc aluminum polyphosphate (ZAPP) pigment on carbon mild steel, Prog. Org. Coatings 94 (2016) 18–27.
[10] A. Ghanbari, M.M. Attar, Surface free energy characterization and adhesion performance of mild steel treated based on zirconium conversion coating: a comparative study, Surf. Coatings Technol. 246 (2014) 26–33.
[11] P. Taheri, K. Lill, J.H.W. De Wit, J.M.C. Mol, H. Terryn, Effects of zinc surface acid-based properties on formation mechanisms and interfacial bonding properties of zirconium-based conversion layers, J. Phys. Chem. C 116 (15) (2012) 8426–8436.
[12] H.E. Mohammadloo, A.A. Sarabi, R.M. Hosseini, M. Sarayloo, H. Sameie, R. Salimi, a comprehensive study of the green Hexafluorozirconic Acid-based conversion coating, Prog. Org. Coatings 77 (2) (2014) 322–330.
[13] L. Fedrizzi, F. Deflorian, P.L. Bonora, corrosion behaviour of fluotitanate pretreated and painted aluminium sheets, Electrochim. Acta 42 (6) (1997) 969–978.
[14] S. Verdier, N. van der Laak, F. Dalard, J. Metson, S. Delalande, An electrochemical and SEM study of the mechanism of formation, morphology, and composition of titanium or zirconium fluoride-based coatings, Surf. Coatings Technol. 200 (9) (2006) 2955–2964.
[15] J.H. Nordlien, J.C. Walmsley, H. Østerberg, K. Nisancioglu, Formation of a zirconium-titanium based conversion layer on aa 6060 aluminium, Surf. Coatings Technol. 153 (1) (2002) 72–78.
[16] F. Andreatta, A. Turco, I. de Graeve, H. Terryn, J.H.W. de Wit, L. Fedrizzi, SKPFM and SEM study of the deposition mechanism of Zr/Ti based pre-treatment on AA6016 aluminum alloy, Surf. Coatings Technol. 201 (18) (2007) 7668–7685.
[17] J. Cerezo, I. Vandendael, R. Posner, K. Lill, J.H.W. de Wit, J.M.C. Mol, H. Terryn, Initiation and growth of Modified Zr-based conversion coatings on multi-metal surfaces, Surf. Coatings Technol. 236 (2013) 284–289.
[18] J. Cerezo, P. Taheri, I. Vandendael, R. Posner, K. Lill, J.H.W. de Wit, J.M.C. Mol, H. Terryn, influence of surface hydroxyls on the formation of Zr-based conversion coatings on AA6014 aluminum alloy, Surf. Coatings Technol. 254 (2014) 277–283.
[19] T. Lostak, A. Maljusch, B. Klink, S. Krebs, M. Kimpel, J. Flock, S. Schulz, W. Schuhmann, Zr-based conversion layer on Zn-Al-Mg alloy coated steel sheets: Insights into the formation mechanism, Electrochim. Acta 137 (2014) 65–74.
[20] O. Lunder, C. Simensen, Y. Yu, K. Nisancioglu, Formation and characterisation of Ti-Zr Based conversion layers on AA6060 aluminium, Surf. Coatings Technol. 184 (2–3) (2004) 278–290.
[21] J. Jolivet, M. Henry, J. Livage, E. Bescher, Metal Oxide Chemistry and Synthesis - From Solution to Solid State, 3th editio, John Wiley & Sons, Inc, 2000.
[22] P.L. Brown, E. Curti, B. Grambow, C. Ekberg, Chem. Thermodynamics Zirconium (2008) 1–512.
[23] S. Verdier, S. Delalande, N. Van Der Laak, J. Metson, F. Dalard, Monochromatized X-Ray photoelectron spectroscopy of the AM60 magnesium alloy surface after treatments in fluoride-based Ti and Zr solutions, Surf. Interface Anal. 37 (5) (2005) 509–516.
[24] A. Clearfield, The mechanism of Hydrolytic Polymerization of Zirconyl solutions, J. Mater. Res. 5 (1) (2016) 161–162.
[25] Y. Gao, Y. Masuda, H. Ohta, K. Koumoto, Room-temperature preparation of ZrO2 precursor thin film in an aqueous peroxozirconium-complex solution, Chem. Mater. (2004) 2615–2622.
[26] P. Puomi, H.M. Fagerholm, J.B. Rosenholm, R. Sipila, Optimization of commercial zirconic acid based pretreatment on hot-dip galvanized and Galfan coated steel, Surf. Coatings Technol. 115 (1999) 79–86.
[27] S.S. Golru, M.M. Attar, B. Ramezanzadeh, Effects of surface treatment of aluminium alloy 1050 on the adhesion and anticorrosion properties of the epoxy coating, Appl. Surf. Sci. (345) (2015) 360–368.
[28] A. Ghanbari, M.M. Attar, The effect of zirconium-based surface treatment on the cathodic disbonding resistance of epoxy coated mild steel, Appl. Surf. Sci. 316 (2014) 429–434.
[29] L.I. Fockaert, P. Taheri, S.T. Abrahami, B. Boelen, H. Terryn, J.M.C. Mol, Zirconium-based conversion film formation on zinc, aluminium and magnesium oxides and their interactions with functionalized molecules, Appl. Surf. Sci. 423 (2017) 817–828.
[30] L.I. Fockaert, S. Pletincx, B. Boelen, T. Hauffman, H. Terryn, J.M.C. Mol, Effect of zirconium-based conversion treatments of zinc, aluminium and magnesium on the chemisorption of ester-functionalized molecules, Appl. Surf. Sci. 508 (2020) 145199–145210.
[31] N.J. Harrick, Study of physics and chemistry of surfaces from frustrated total internal reflections, Phys. Rev. Lett. 4 (5) (1960) 224–226.
[32] M. Öhman, D. Persson, An integrated in situ ATR-FTIR and EIS set-up to study buried metal – polymer interfaces exposed to an electrolyte solution, Electrochim. Acta 52 (2007) 5159–5171.
[33] M. Öhman, D. Persson, C. Leygraf, In situ ATR-FTIR Studies of the aluminium / polymer interface upon exposure to water and electrolyte, Prog. Org. Coatings 57 (2006) 78–88.
[34] M. Öhman, D. Persson, ATR-FTIR kretschmann spectroscopy for interfacial studies of a hidden aluminum surface coated with a silane film and epoxy I. characterization by IRRAS and ATR-FTIR, Surf. Interface Anal. 44 (2) (2012) 133–143.
[35] M. Öhman, D. Persson, D. Jacobsson, In situ studies of conversion coated zinc / polymer surfaces during exposure to corrosive conditions, Prog. Org. Coatings 70 (2011) 16–22.
[36] P. Taheri, H. Terryn, J.M.C. Mol, Studying interfacial bonding at buried polymer–Zinc interfaces, Prog. Org. Coatings 89 (2015) 323–331.
[37] P. Taheri, P. Laha, H. Terryn, J.M.C. Mol, An in situ study of zirconium-based conversion treatment on zinc surfaces, Appl. Surf. Sci. 356 (2015) 837–843.
[38] S. Pletincx, J.M.C. Mol, H. Terryn, A. Hubin, T. Hauffman, An in situ spectro-electrochemical monitoring of aqueous effects on polymer / metal oxide interfaces, J. Electroanal. Chem. 848 (2019) 113311 11327.
[39] L.I. Fockaert, S. Pletincx, D. Ganzinga-Jurg, B. Boelen, T. Hauffman, H. Terryn, J.M.C. Mol, Chemisorption of polyester coatings on zirconium-based conversion coated multi-metal substrates and their stability in aqueous environment, Appl. Surf. Sci. 508 (2020) 144771–144781.
[40] a. Leng, H. Streckel, M. Stratmann, The delamination of polymeric coatings from steel. Part 2: first stage of delamination, effect of type and concentration of cations on delamination, chemical analysis of the interface, Corros. Sci. 41 (3) (1999) 579–597.
[41] a. Leng, H. Streckel, M. Stratmann, The delamination of polymeric coatings from steel. Part 1: calibration of the kelvinprobe and basic delamination mechanism, Corros. Sci. 41 (3) (1999) 547–578.
[42] M. Sababi, H. Terryn, J.M.C. Mol, The influence of a Zr-based conversion treatment on interfacial bonding strength and stability of Epoxy Coated Carbon Steel, Prog. Org. Coatings 105 (2017) 29–36.
[43] C. Stromberg, P. Thissen, I. Klueppel, N. Fink, G. Grundmeier, synthesis and characterisation of surface gradient thin conversion films on zinc coated steel, Electrochim. Acta 52 (2006) 804–815.
[44] T. Lostak, S. Krebs, A. Maljusch, T. Gothe, M. Giza, M. Kimpel, J. Flock, S. Schulz, Formation and characterization of Fe3+ /Cu2+ modified zirconium oxide conversion layers on zinc alloy coated steel sheets, Electrochim. Acta 112 (2013) 14–23.
[45] F. Andreatta, A. Lanzutti, L. Paussa, L. Fedrizzi, addition of phosphates or copper nitrate in a fluotitanate conversion coating containing a silane coupling agent for aluminium alloy, Prog. Org. Coatings 77 (12) (2014) 2107–2115.
[46] P.D. Deck, M. Moon, R.J. Sujdak, investigation of fluoacid based conversion coatings on aluminum, Prog. Org. Coatings 34 (1998) 39–48.
[47] H.L. Faigen, Method for Treating Metal Surfaces With Compositions Comprising Zirconium and a Polymer, (1975), p. 3912548.
[48] U. Karmaschek, R. Mady, Chromium-Free Process for the No-Rinse Treatment of Aluminium and Its Alloys and Aqueous Bath Solution Suitable for This Process, (1999), p. 5868872.
[49] W.E. Fristad, J. Liang, T.S. Kelly, Coating Composition. US7063735B, (2006).
[50] S. Sander, Lothar, E.M. Musingo, W.J. Neill, Composition and Method for Non-Chromate Coating of Aluminium, (1990), p. 4921552.
[51] W. Wichelhaus, B. Schenzie, H. Quellhorst, Methos for Providing Metal Surfaces With Protection Against Corrosion. 0150524A1, (2003).
[52] M.A. Smit, J.A. Hunter, J.D.B. Sharman, G.M. Scamans, J.M. Sykes, Effect of organic additives on the performance of titanium-based conversion coatings, Corros. Sci. 45 (9) (2003) 1903–1920.
[53] H. Assi, G. Mouchaham, N. Steunou, T. Devic, C. Serre, Titanium coordination compounds : from discrete metal complexes to metal – organic frameworks, Chem.

Soc. Rev. 46 (2017) 3431–3452.
[54] Y. Bai, Y. Dou, L. Xie, W. Rutledge, J. Li, H. Zhou, Zr-based metal–organic frameworks: design, synthesis, structure, and applications, Chem. Soc. Rev. 45 (2016) 2327–2367.
[55] D.K. Owens, R.C. Wendt, Estimation of the surface free energy of polymers, J. Appl. Polym. Sci. 13 (1969) 1741–1747.
[56] S. Pletincx, L.L.I. Fockaert, J.M.C. Mol, T. Hauffman, T. Herman, Probing the formation and degradation of chemical interactions from model molecule / metal oxide to buried polymer / metal oxide interfaces, Npj Mater. Degrad. 3 (23) (2019) 1–12.
[57] N. Fink, B. Wilson, G. Grundmeier, Formation of ultra-thin amorphous conversion films on zinc alloy coatings: part 1. composition and reactivity of native oxides on ZnAl (0.05%) coatings, Electrochim. Acta 51 (14) (2006) 2956–2963.
[58] C.D. Wagner, R.H. Raymond, L.H. Gale, Empirical atomic sensitivity factors for quantitative analysis by Electron spectroscopy for chemical analysis, Surf. Interface Anal. 3 (5) (1981) 211–225.
[59] G.C. Smith, Evaluation of a simple correction for the hydrocarbon contamination layer in quantitative surface analysis by XPS, J. Electron Spectros. Relat. Phenomena 148 (2005) 21–28.
[60] C.J. Powell, A. Jablonski, I.S. Tilinin, S. Tanuma, D.R. Penn, Surface sensitivity of X-Ray photoelectron spectroscopy, J. Electron Spectros. Relat. Phenomena 98–99 (1999) 1–15.
[61] F.M. Fowkes, Attractive forces at interfaces, Ind. Eng. Chem. 5 (1964) 40–52.
[62] George Socrates, Infrared and Raman Characteristic Group Frequencies, third edit., John Wiley & Sons, Inc, 2001.
[63] Coates, J. Encyclopedia of Analytical Chemistry, Interpretation of Infrared Spectra, A Practical Approach; Meyers, R. A., Ed.; John Wiley & Sons, Ltd.
[64] S. Pletincx, L. Trotochaud, L.-L. Fockaert, J.M.C. Mol, A.R. Head, O. Karslıoğlu, H. Bluhm, H. Terryn, T. Hauffman, In situ characterization of the initial effect of water on molecular interactions at the interface of Organic/Inorganic hybrid systems, Sci. Rep. 7 (2017) 45123.
[65] S. Pletincx, K. Marcoen, L. Trotochaud, L.-L. Fockaert, J.M.C. Mol, A.R. Head, O. Karslioğlu, H. Bluhm, H. Terryn, T. Hauffman, Unravelling the chemical influence of water on the PMMA/Aluminum oxide hybrid interface in situ, Sci. Rep. 7 (1) (2017) 13341.
[66] Y.T. Tao, structural comparison of self-assembled monolayers of n-Alkanoic Acids on the surfaces of silver, copper, and aluminum, J. Am. Chem. Soc. 115 (10) (1993) 4350–4358.
[67] S. Hofmann, G. Zhou, J. Kovac, S. Drev, S.Y. Lian, B. Lin, Y. Liu, J.Y. Wang, Preferential sputtering effects in depth profiling of multilayers with SIMS, XPS and AES, Appl. Surf. Sci. 483 (2019) 140–155.
[68] D.R. Baer, M.H. Engelhard, A.S. Lea, P. Nachimuthu, T.C. Droubay, J. Kim, B. Lee, C. Mathews, R.L. Opila, L.V. Saraf, et al., Comparison of the sputter rates of oxide films relative to the sputter rate of SiO2, J. Vac. Sci. Technol. A 28 (5) (2010) 1060.
[69] G.B. Deacon, F. Huber, R.J. Phillips, Diagnosis of the nature of carboxylate coordination from the direction of shifts of carbon-oxygen stretching frequencies, Inorganica Chim. Acta 104 (1985) 41–45.
[70] G.B. Deacon, R.J. Phillips, Relationships between the carbon-oxygen stretching frequencies of carboxylato complexes and the type of carboxylate coordination, Rev. Chem. 33 (1980) 227–250.
[71] L.I. Fockaert, T. Würger, R. Unbehau, B. Boelen, R.H. Meißner, S.V. Lamaka, M.L. Zheludkevich, H. Terryn, J.M.C. Mol, ATR-FTIR in kretschmann configuration integrated with electrochemical cell as in situ interfacial sensitive tool to study corrosion inhibitors for magnesium substrates, Electrochim. Acta 345 (2020) 136166.